

Systemic Anti–Hepatocyte Growth Factor Monoclonal Antibody Therapy Induces the Regression of Intracranial Glioma Xenografts

K. Jin Kim,¹ Lihong Wang,¹ Yi-Chi Su,¹ G. Yancey Gillespie,² Amandeep Salhotra,³ Bachchu Lal,³ and John Laterra³

Abstract Purpose: Hepatocyte growth factor (HGF) and its receptor Met are involved in the initiation, progression, and metastasis of numerous systemic and central nervous system tumors. Thus, an anti-HGF monoclonal antibody (mAb) capable of blocking the HGF-Met interaction could have broad applicability in cancer therapy.

Experimental Design: An anti-HGF mAb L2G7 that blocks binding of HGF to Met was generated by hybridoma technology, and its ability to inhibit the various biological activities of HGF was measured by *in vitro* assays. The ability of L2G7 to inhibit the growth of tumors was determined by establishing s.c. and intracranial xenografts of human U87 and U118 glioma cell lines in nude mice, and treatment with 100 µg of L2G7 or control given i.p. twice per week.

Results: MAb L2G7 strongly inhibited all biological activities of HGF measured *in vitro*, including cell proliferation, cell scattering, and endothelial tubule formation. Treatment with L2G7 completely inhibited the growth of established s.c. xenografts in nude mice. Moreover, systemic administration of L2G7 from day 5 induced the regression of intracranial U87 xenografts and dramatically prolonged the survival of tumor-bearing mice from a median of 39 to >90 days. L2G7 treatment of large intracranial tumors (average tumor size, 26.7 mm³) from day 18 induced substantial tumor regression (control group, 134.3 mm³; L2G7 treated group, 11.7 mm³) by day 29 and again prolonged animal survival.

Conclusions: These findings show that blocking the HGF-Met interaction with systemically given anti-HGF mAb can have profound antitumor effects even within the central nervous system, a site previously believed to be resistant to systemic antibody-based therapeutics.

Hepatocyte growth factor (HGF) is a multifunctional heterodimeric protein typically produced by mesenchymal cells. HGF mediates mitogenesis, morphogenesis, angiogenesis, and cytoprotection of various cell types (1, 2). The pleiotropic activities of HGF are mediated through its cellular receptor, a transmembrane tyrosine kinase encoded by the proto-oncogene Met. During embryonic development, HGF and its receptor Met play important roles in mesenchymal-

epithelial interactions required for organ formation, liver development, and neural differentiation (3, 4). However, in adults, the normal physiologic role of HGF and Met may be limited to tissue regeneration and wound healing (3–5). HGF and Met are coexpressed and often overexpressed in a broad spectrum of human solid tumors including lung, breast, and brain (1, 6), and HGF acts as an autocrine and/or paracrine growth factor for these tumor cells (7). Blocking the HGF-Met interaction by genetic modulation, or by NK4 from the α -subunit of HGF, significantly inhibits the growth of human tumors in xenograft mouse models (8–10).

Recently, monoclonal antibodies (mAb) to growth factors or their receptors have begun to play an increasingly important role in cancer therapy. Currently marketed mAbs that directly or indirectly inhibit tumor cell growth include trastuzumab (Herceptin), a mAb directed to the HER2 receptor; cetuximab (Erbix), an anti-epidermal growth factor receptor mAb; and bevacizumab (Avastin), an antiangiogenesis mAb that neutralizes vascular endothelial growth factor (VEGF). However, to similarly inhibit tumor growth in a xenograft model, Cao et al. (11) needed a combination of three anti-HGF mAbs, and suggested that the complex heterodimeric structure of HGF makes it necessary to simultaneously target multiple HGF epitopes by combining mAbs, a difficult approach for drug development. In this study, we show that a single blocking

Authors' Affiliations: ¹Galaxy Biotech, LLC, Mountain View, California; ²Division of Neurosurgery, University of Alabama at Birmingham, Birmingham, Alabama; and ³Department of Neurology, The Kennedy Krieger Research Institute and The Johns Hopkins University School of Medicine, Baltimore, Maryland

Received 8/15/05; revised 11/10/05; accepted 11/30/05.

Grant support: NIH grants 1R43CA101283-01A1 (K.J. Kim) and RO1 NS32148 (J. Laterra).

The costs of publication of this article were defrayed in part by the payment of page charges. This article must therefore be hereby marked *advertisement* in accordance with 18 U.S.C. Section 1734 solely to indicate this fact.

Note: L. Wang and Y.-C. Su contributed equally to this work.

Requests for reprints: K. Jin Kim, Galaxy Biotech, LLC, 2462 Wyandotte Street, Mountain View, CA 94033. Phone: 650-964-4966, ext. 214; Fax: 650-694-7717; E-mail: kjinkim@msn.com.

©2006 American Association for Cancer Research.
doi:10.1158/1078-0432.CCR-05-1793

anti-HGF mAb, L2G7, can inhibit various biological activities induced by HGF *in vitro*, and has profound antitumor activities even within the central nervous system (CNS).

Materials and Methods

Production of HGF-Flag and Met-Fc. DNAs encoding recombinant human HGF and HGF-Flag (Flag peptide linked to the COOH terminus of HGF) were constructed in a pDisplay expression vector (Invitrogen, Carlsbad, CA) and expressed by transfecting EcR-293 human kidney fibroblast cells as previously described (12). HGF and HGF-Flag were prepared by treating transfected cells with 4 $\mu\text{mol/L}$ of Ponasterone A (Invitrogen) for 4 to 5 days in DMEM with or without 2% FCS. The amount of HGF-Flag secreted into the culture supernatant was determined using a mAb-based HGF-specific ELISA with commercially available HGF (R&D Systems, Minneapolis, MN) as a standard. Met-Fc fusion protein for use in assays was prepared similarly using a vector with DNA encoding residues 1 to 929 of the extracellular domain of human Met linked to the Fc portion of human IgG₁ (residues 216-446). The amount of Met-Fc secreted was determined using an anti-hlgG capture ELISA with human IgG as a standard. The bioactivities of HGF and HGF-Flag were confirmed in an HGF/Met binding ELISA and other *in vitro* bioassays described below, and the bioactivity of Met-Fc was confirmed by its ability to block the activity of HGF in these assays.

Generation of mAbs. BALB/c mice were immunized in each hind footpad at least 10 times at 1 week intervals, with 1 to 2 μg of HGF (PeproTech, Rocky Hill, NJ, or produced as described above) resuspended in MPL-TDM (Sigma-Aldrich, St. Louis, MO). Hybridomas were generated by fusing splenic lymph node cells with murine myeloma cells, P3X63AgU.1 (American Type Culture Collection, Manassas, VA) as previously described (13). The HGF binding ability of mAbs secreted by the hybridomas was determined in an HGF binding ELISA and an HGF-Flag capture ELISA, and blocking activity of selected mAbs was determined in the HGF-Flag/Met-Fc binding ELISA, as described below. Selected hybridomas were cloned twice by limiting dilution. The isotypes of mAbs were determined using an isotyping kit (Zymed Laboratories/Invitrogen). Ascites were raised and antibodies were purified using ImmunoPure (A/G) IgG (Pierce, Rockford, IL).

ELISAs. Each step of the assay was carried out by room temperature incubation with the appropriate reagent for 1 hour, except that the initial antigen coating step was done overnight at 4°C. Between each step, plates were washed thrice in PBS containing 0.05% bovine serum albumin (BSA) and 0.05% Tween 20. For the HGF binding ELISA, plates were coated with 0.5 $\mu\text{g/mL}$ of HGF, blocked with 2% skimmed milk and incubated with hybridoma culture supernatant, followed by the addition of horseradish peroxidase (HRP) goat anti-mouse IgG and then TMB substrate (Sigma-Aldrich). For the HGF-Flag capture ELISA, plates were coated with 2 $\mu\text{g/mL}$ of goat anti-mouse IgG-Fc, blocked with 2% BSA and incubated with various concentrations of mAbs, followed by the addition of HGF-Flag (0.2 $\mu\text{g/mL}$) plus mouse IgG (20 $\mu\text{g/mL}$). The bound HGF-Flag was detected with HRP-M2 anti-Flag mAb (Invitrogen) and substrate. For the Met-Fc/HGF-Flag binding ELISA, plates were coated with 2 $\mu\text{g/mL}$ of goat anti-human IgG-Fc, blocked with 2% BSA and incubated with Met-Fc (1 $\mu\text{g/mL}$). The unoccupied goat anti-Fc binding sites were blocked by incubation with 5 $\mu\text{g/mL}$ of human IgG. Wells were then incubated with HGF-Flag (0.2 $\mu\text{g/mL}$) plus mAbs. The bound HGF-Flag was detected with HRP-M2 anti-Flag mAb and substrate.

Madin-Darby canine kidney cell scattering assay. The assay was done using Madin-Darby canine kidney cells (obtained from American Type Culture Collection) as described (11). Briefly, Madin-Darby canine kidney cells (10^3 cells/100 μL /well) in DMEM supplemented with 5% FCS were stimulated with 50 ng/mL HGF with or without various concentrations of mAbs for 2 days at 37°C. Cells were then washed in PBS, fixed in 2% formaldehyde and stained with 0.5% crystal

violet in 50% ethanol (v/v) for 10 minutes at room temperature. Scattering activity was determined by microscopic examination and photography.

Proliferation assays. The assay using Mv 1 Lu mink lung epithelial cells (CCL-64 from American Type Culture Collection) was done as described (14). Briefly, Mv 1 Lu cells (2×10^4 cells/100 μL /well) grown in DMEM containing 10% FCS were resuspended in serum-free DMEM and stimulated with 100 μL /well of HGF (20 ng/mL) plus transforming growth factor- β 1 (1 ng/mL, R&D Systems) and various concentrations of L2G7 or control mAb (mouse IgG_{2a}) for 24 hours. The level of cell proliferation was determined by the addition of WST-1 (Roche Applied Science, Indianapolis, IN) for 16 hours. For the assay using human umbilical vascular endothelial cells (HUVEC; Cambrex, East Rutherford, NJ), cells were grown in EMB-2 endothelial growth medium containing 10% FCS plus endothelial cell growth supplements provided by Cambrex. HUVEC (5×10^3 cells/100 μL /well) were cultured in EMB-2/1% FCS for 24 hours, in EMB-2/0.1% FCS for 24 hours and then in EMB-2/0.1% FCS containing HGF (20 ng/mL) +/- L2G7 mAb for 48 hours. The level of cell proliferation was determined by the addition of ^3H -thymidine for 16 hours.

Endothelial tubule assay. The assay was done as previously described (15) with modifications. Ice-cold Matrigel (BD Biosciences, San Jose, CA) and HUVEC (3×10^6 cells/mL) in DMEM were mixed together at a 4:1 ratio, and 100 μL of the mixture was added to each well. After gelation at 37°C for 30 minutes, the wells were overlaid with 100 μL /well of EBM-2/0.1% FCS/0.1% BSA with or without 200 ng/mL of HGF and 20 $\mu\text{g/mL}$ of L2G7. After incubation at 37°C for 48 hours, cells were fixed in 4% formaldehyde for 30 minutes at room temperature, washed in PBS and stained using toluidine blue. Tubule formation was observed by microscopy at $\times 40$ magnification.

Apoptosis assay. The assay was done as described (16) with modifications. U87 cells (3×10^3 cells/100 μL /well) were incubated in DMEM/10% FCS for 24 hours and then in 100 μL of DMEM/0.1% FCS containing 50 ng/mL HGF with or without L2G7 (5 $\mu\text{g/mL}$) or control antibody for 24 hours. The cells were then incubated with 40 ng/mL of anti-Fas agonist antibody CH-11 (Upstate, Waltham, MA) in DMEM/0.1% BSA for 48 hours, followed by the addition of WST-1 for 1 hour to determine cell viability. Experiments were done in triplicate.

Subcutaneous xenograft mouse model. Experiments were carried out as previously described (17). Female 4- to 6-week-old NIH III Xid/Beige/Nude mice (Charles River Laboratories, Wilmington, MA) were injected s.c. with 5×10^6 cells in 0.1 mL of PBS in the dorsal areas. When the tumor size reached $\sim 50 \text{ mm}^3$, the mice were randomly divided into groups ($n = 6$ per group) and injected with L2G7 or control mAb (typically 100 μg) i.p. twice weekly in a volume of 0.1 mL PBS. Tumor volumes were determined weekly by measuring two dimensions [length (a) and width (b)] and calculating volume as $V = ab^2 / 2$. At the end of each experiment, tumors were excised and weighed.

Intracranial xenograft model. Experiments were done as previously described (8). C.B-17 Scid/Beige mice were anesthetized by i.p. injection of ketamine (100 mg/kg) and xylazine (5 mg/kg), and U87 tumor cells (10^5 cells/5 μL per animal) were injected stereotactically into the caudate/putamen. Starting at the indicated times, 100 μg ($\sim 5 \text{ mg/kg}$) of mAb L2G7 or control mAb was given i.p. twice per week. Groups of mice ($n = 5$) were sacrificed at the indicated times and the brains were removed for histologic studies. The remaining mice ($n = 10$) were monitored for survival. Tumor volumes were quantified by measuring tumor cross-sectional areas on H&E-stained cryostat sections from perfusion-fixed brains using computer-assisted image analysis as previously described (8). All animal protocols used in this study were approved by the respective institutional Institutional Animal Care and Use Committee.

Immunohistochemistry. Cryostat 10- μm -thick sections of brain taken from mice on day 29, following treatment with three 100- μg doses of L2G7 or control mAb given twice weekly from day 18, were stained with antibodies to cleaved caspase-3 (Cell Signaling Technology,

Beverly, MA), anti-Ki67 antibodies (DakoCytomation, Carpinteria, CA), and anti-laminin antibodies (Life Technologies/Invitrogen) to detect apoptotic cells, proliferating cells, and blood vessels, respectively, as previously described (8). The bound primary antibodies were detected using HRP-conjugated secondary antibodies, followed by the addition of 3,3'-diaminobenzidine peroxidase substrate, counterstained with Gill's hematoxylin solution. Apoptotic proliferation and angiogenesis indices were determined using computer-assisted image analysis as previously described (8).

Statistical analysis. The *in vitro* apoptosis data and the quantitative histologic and immunohistochemical data from intracranial tumors were analyzed using ANOVA followed by a post hoc Fisher's PLSD test. Survival studies were analyzed with Kaplan-Meier.

Results

Generation of a blocking anti-HGF mAb. To develop a single, fully neutralizing anti-HGF mAb, we extensively immunized BALB/c mice with recombinant human HGF by footpad injections and generated from seven fusions of ~3,500 hybridomas secreting anti-HGF mAbs. Chimeric proteins consisting of HGF fused to Flag peptide (HGF-Flag), and the Met extracellular domain fused to the human IgG₁ Fc region (Met-Fc), were produced by conventional recombinant techniques and used to determine the ability of these mAbs to inhibit the binding of HGF to its Met receptor. Figure 1A shows the ability of three separate anti-HGF mAbs, each recognizing a different epitope (data not shown), to capture HGF in solution. Although the IgG_{2a} mAb L2G7 has intermediate affinity for HGF as judged by binding ability, it is the only mAb identified that completely blocks the binding of HGF-Flag to Met-Fc in an ELISA (Fig. 1B). The mAb L2G7 is specific for HGF, as it shows no binding to other growth factors such as VEGF, fibroblast growth factor, or epidermal growth factor (data not shown).

Anti-HGF mAb L2G7 neutralizes all tested biological activities of HGF *in vitro*. The ability of mAb L2G7 to block HGF binding to Met suggested that it would inhibit all HGF-induced cell responses, but this supposition required verification because the α - and β -subunits of HGF mediate different

activities (18–20). One important bioactivity of HGF mediated through its α -subunit, from which its alternate name "scatter factor" derives, is the ability to induce cell scattering. Thus, we determined the effect of various concentrations of L2G7 on the HGF-induced scattering of Madin-Darby canine kidney epithelial cells, a widely used biological assay for quantifying HGF scatter activity. We observed clear inhibition of scattering at a 5:1 molar ratio of L2G7 mAb to HGF (data not shown), and Fig. 2A shows the result obtained at a higher 100:1 molar ratio of L2G7 to HGF. A key biological activity of HGF mediated through its β -subunit is mitogenesis of certain cell types. Figure 2B shows that L2G7 at a 0.3:1 molar ratio of mAb to HGF already strongly inhibits HGF-induced proliferation of Mv 1 Lu mink lung epithelial cells, and 80% to 90% inhibition is achieved at molar ratios of 1:1 or higher. Thus, mAb L2G7 blocks HGF-induced biological activities attributable to both the α - and β -HGF subunits.

Angiogenesis is required for the growth of solid tumors. HGF is a potent angiogenic factor (21), and tumor levels of HGF correlate with the vascular density of human malignancies including gliomas (22). HGF can also stimulate the production of other angiogenic factors such as VEGF and can potentiate VEGF-induced angiogenesis (15, 23). Two early steps involved in angiogenesis are endothelial cell proliferation and tubule formation. We therefore determined the effect of L2G7 on HGF-induced proliferation of HUVEC and on formation of vessel-like tubules in three-dimensional collagen gels. Stimulation of HUVEC proliferation by HGF (20 ng/mL, 48 hours) was completely inhibited by L2G7 even at a 1:1 mAb to HGF molar ratio (Fig. 2B). HUVECs suspended in three-dimensional collagen gels developed an interconnected branching tubule network after stimulation with HGF (200 ng/mL, 48 hours), whereas cells treated with HGF plus L2G7 showed little or no such tubule formation (Fig. 2C). Hence, L2G7 blocks HGF-induced proliferative and morphogenic aspects of angiogenesis.

HGF protects tumor cells from apoptotic death induced by numerous modalities including DNA-damaging agents commonly used in cancer therapy (24, 25). The majority of human malignant glioma cells express the death receptor Fas, making them susceptible to apoptosis induced by anti-Fas antibody *in vitro* (26). Thus, we determined the effects of L2G7 on HGF-mediated cytoprotection of U87 glioma cells treated with apoptotic anti-Fas mAb CH-11. U87 cell viability after CH-11 treatment (24 hours) was reduced to ~45% of that in untreated controls, an effect that was completely reversed by preincubating cells with HGF in the presence of an irrelevant control antibody but not by HGF in the presence of L2G7 (Fig. 2D; $P < 0.0001$ for control antibody versus L2G7).

Effects of anti-HGF mAb L2G7 on the growth of gliomas in subcutaneous xenograft mouse models. The ability of L2G7 to block the multiple tumor-promoting activities of HGF suggests that this mAb may have antitumor activity. To select tumor models for *in vivo* studies, we examined several glioma tumor cell lines for their membrane expression of Met and for HGF secretion, using flow cytometric analysis and anti-HGF-specific ELISA, respectively. Three glioma tumor cell lines, U87, U118, and U251, were chosen for our studies because U87 and U118 expressed membrane Met and secreted significant levels of HGF (~20–35 ng/mL in 7-day-old confluent culture supernatant),

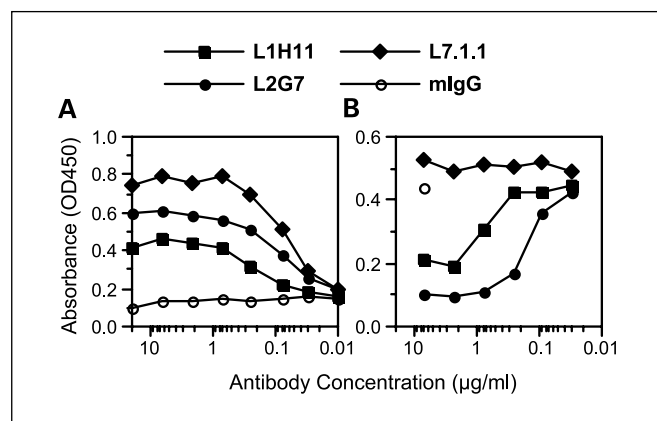


Fig. 1. Binding and blocking activities of anti-HGF mAbs measured by ELISA. **A**, for binding, mAbs were captured onto a goat anti-mouse IgG-coated ELISA plate and incubated with HGF-Flag (0.5 µg/mL), followed by HRP-M2 anti-Flag mAb (Invitrogen). **B**, for blocking of HGF-Flag to Met-Fc binding, plates were coated with goat anti-human IgG-Fc and incubated with Met-Fc (1 µg/mL), and then with HGF-Flag (0.2 µg/mL) ± anti-HGF mAbs. The bound HGF-Flag was detected with HRP-M2 anti-Flag mAb.

whereas U251 expressed a high level of membrane Met but did not secrete HGF.

We then determined the antitumor effect of L2G7 in preestablished s.c. xenograft nude mouse models. L2G7 was given i.p. twice weekly after tumor sizes had reached $\sim 50 \text{ mm}^3$ as described (17). At $100 \mu\text{g}$ ($\sim 5 \text{ mg/kg}$) per injection, L2G7 completely inhibited the growth of U118 tumors (Fig. 3A). In the U87 xenograft model, either 50 or $100 \mu\text{g}$ L2G7 per

injection not only inhibited tumor growth but actually caused tumor regression (Fig. 3B). Control mAb ($100 \mu\text{g/injection}$) only slightly inhibited tumor growth compared with PBS control. In separate experiments, we investigated effects in xenograft models of 5 or $10 \mu\text{g}$ per injection of the mouse-human chimeric mAb ChL2G7, which we constructed by standard recombinant methods. We observed complete U87 tumor growth inhibition with doses of ChL2G7 as low as $10 \mu\text{g}$ per injection, and $\sim 75\%$ growth inhibition at the $5 \mu\text{g}$ dose level (data not shown). In contrast to the U87 and U118 cell lines that secrete HGF, L2G7 had no effect on the growth of Met+/HGF- U251 glioma tumor xenografts (Fig. 3C), confirming that L2G7 blocks tumor growth by specifically inhibiting HGF.

Effects of anti-HGF mAb L2G7 on the growth of intracranial glioma xenografts. Although the results in s.c. glioma xenografts were encouraging, it was necessary to assess efficacy using an orthotopic tumor model because unique features of the CNS site, such as the "blood-brain barrier," could present obstacles to systemic mAb therapy (27). The previously observed inefficacy of systemic antibody therapies against CNS tumors has been attributed to restricted vascular permeability even for CNS metastases, despite their characteristically highly permeable tumor vasculature (28, 29). However, the specific nature of the targeted antigen and the potency of the blocking antibody are likely to strongly influence the efficacy of mAb therapy against CNS malignancies. Thus, L2G7 efficacy was examined in mice bearing preestablished intracranial U87 glioma xenografts. L2G7 ($100 \mu\text{g/injection}$, i.p., twice weekly) given from days 5 to 52, significantly prolonged animal survival (Fig. 4A; $P < 0.0001$). In control mice, median survival was 39 days and all mice died from progressive tumors by day 41. In contrast, all mice treated with L2G7 survived to day 70, and 80% survived to day 90, 6 weeks after cessation of mAb treatment (Fig. 4A). In sacrificed mice, on day 21 after treatment with three doses of L2G7 or PBS, control tumors were >10 -fold larger than L2G7-treated tumors (6.6 ± 2.7 versus $0.54 \pm 0.17 \text{ mm}^3$; Fig. 4B). L2G7-treated animals remaining alive on day 91 were sacrificed and examined for tumor burden. The brains were found to have tumors consistent with tumor regrowth after withdrawal of L2G7 therapy.

To test the mAb efficacy under more stringent conditions, in a similar experiment initiation of L2G7 treatment was delayed until day 18. A subset of mice ($n = 5$) were sacrificed immediately before starting therapy and 11 days later after three doses of L2G7 had been given. Tumor volumes were quantified by measuring tumor cross-sectional areas of H&E stained brain sections using computer-assisted image analysis. L2G7 induced substantial tumor regression (Fig. 4C and D; $P = 0.03$). Specifically, pretreatment tumor volumes on day 18 were $26.7 \pm 2.5 \text{ mm}^3$ (range, 19.5 - 54 mm^3 ; median, 27.9 mm^3). On day 29, after three doses of L2G7, tumors were only $11.7 \pm 5.0 \text{ mm}^3$ (range, 0 - 26.2 mm^3 ; median, 7.5 mm^3). On day 29, tumor volumes from mice treated with isotype-matched control mAb were $134.3 \pm 22.0 \text{ mm}^3$ (range, 71.2 - 196.8 mm^3 ; median, 128 mm^3). Hence, tumors treated with control mAb grew 5-fold with a mean volume 12 times larger than the L2G7-treated tumors ($P < 0.001$). In the mice that were not sacrificed ($n = 10$), median survival in the control mice was 32 days and all died by day 42, whereas none of

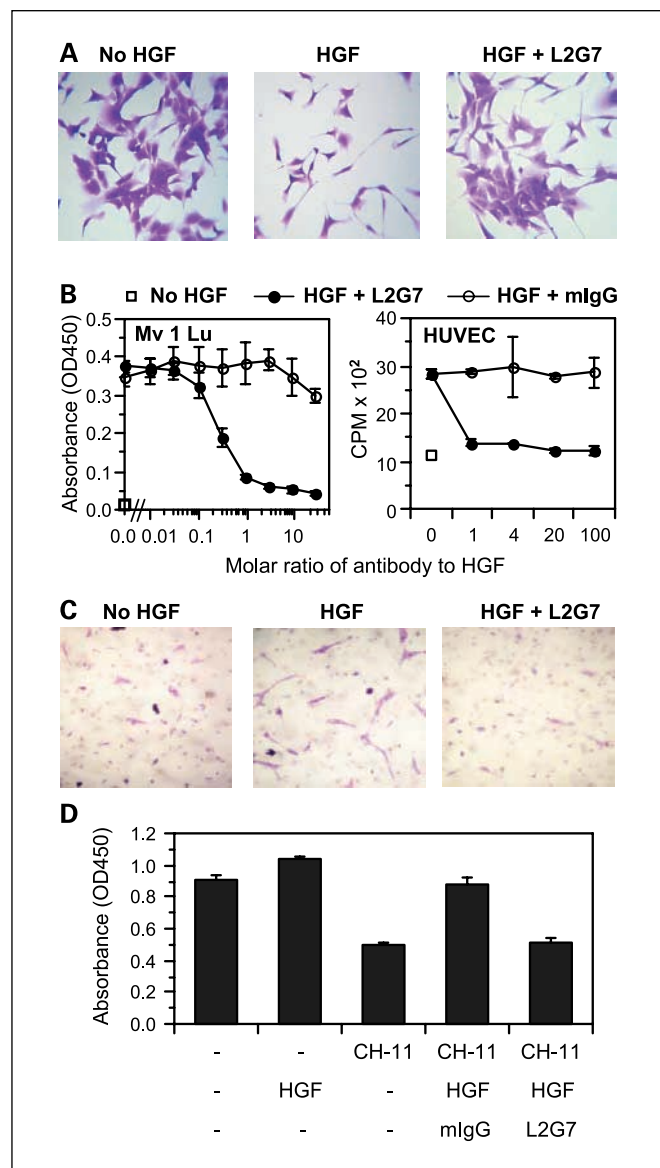


Fig. 2. Blocking effects of mAb L2G7 on the scattering, mitogenic, angiogenic, and antiapoptotic activities of HGF. *A*, Madin-Darby canine kidney cells were stimulated with 50 ng/mL of HGF $\pm 10 \mu\text{g/mL}$ L2G7 for 2 days. Cells were stained with crystal violet ($\times 100$ magnification). *B*, Mv1 Lu mink lung epithelial cells and HUVEC were each incubated with or without HGF (20 ng/mL) and L2G7 or isotype-matched control mAb (mIgG) for 24 and 48 hours, respectively, and the level of cell proliferation was determined by the addition of WST-1 or ^3H -thymidine, respectively (points, mean; bars, \pm SD). *C*, HUVEC in DMEM/gel were overlaid with or without 200 ng/mL of HGF $\pm 20 \mu\text{g/mL}$ of L2G7 for 48 hours. Cells were fixed and stained using toluidine blue, and tubule formation was determined by microscopic examination ($\times 40$ magnification). *D*, U87 tumor cells were incubated with or without HGF (50 ng/mL) \pm mAb L2G7 ($5 \mu\text{g/mL}$) or mIgG for 24 hours and then with anti-Fas mAb CH-11 (40 ng/mL) for 48 hours, and cell viability was determined by the addition of WST-1 (points, mean; bars, \pm SD).

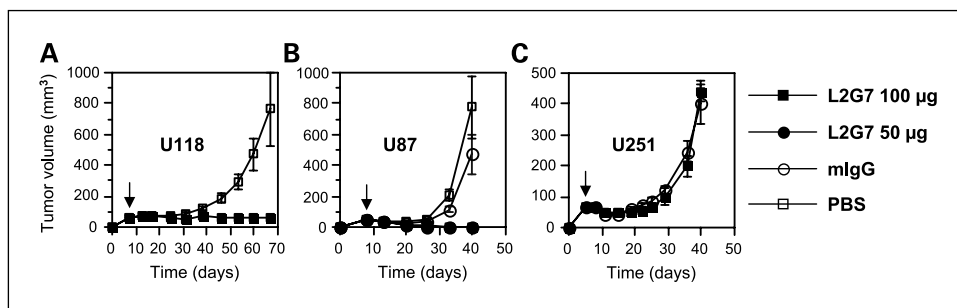


Fig. 3. Inhibition or regression of s.c. glioma xenografts by L2G7. U118 (A), U87 (B), and U251 (C) glioma tumor cells were implanted s.c. into NIH III Beige/Nude mice. After tumor size had reached ~50 mm³, groups of mice (n = 6) were treated i.p. twice weekly with 50 or 100 µg L2G7 or 100 µg isotype-matched control mAb (mIgG) or PBS as indicated; arrows, first day of treatment; points, mean; bars, ±SE.

the L2G7-treated mice died until day 46, and L2G7 extended median survival to day 61 ($P < 0.0001$; not shown). Thus, L2G7 induced tumor regression in mice with very high tumor burdens but did not prolong survival indefinitely. This experiment also indicates that the efficacy of L2G7 is not dependent on injury at the tumor cell injection site, because by the time therapy was initiated on day 18, the small injection site injury had healed. Noninvasive imaging of intracranial tumors established with firefly luciferase-transfected U87 cells similarly showed that 1 week of L2G7 therapy reduced tumor volumes by ~80% (data not shown). L2G7 had no significant

effect on the survival of mice bearing firefly luciferase-transfected D54 glioma intracranial xenografts which do not secrete HGF (data not shown), again demonstrating the HGF-specific action of L2G7.

Mechanisms of antitumor activity of anti-HGF mAb L2G7. A detailed analysis of histologic sections of intracranial tumors was done to investigate the potential mechanisms of the antitumor effects of L2G7 (Fig. 5). On day 29, following three 100-µg doses of L2G7 given twice weekly from day 18, tumor cell proliferation (Ki-67 index) and angiogenesis (vessel density) were reduced by 51% ($P < 0.0001$) and 62% ($P < 0.001$), respectively, whereas the apoptotic index of tumor cells quantified by the number of activated caspase-3-positive cells was increased 6-fold ($P < 0.0001$). These results suggest that the potent antitumor effects of L2G7 are due to its ability to inhibit several HGF activities required for tumor cell proliferation and survival. In particular, the pronounced tumor regression that occurred soon after initiating L2G7 therapy may be indicative of an apoptotic cell death response.

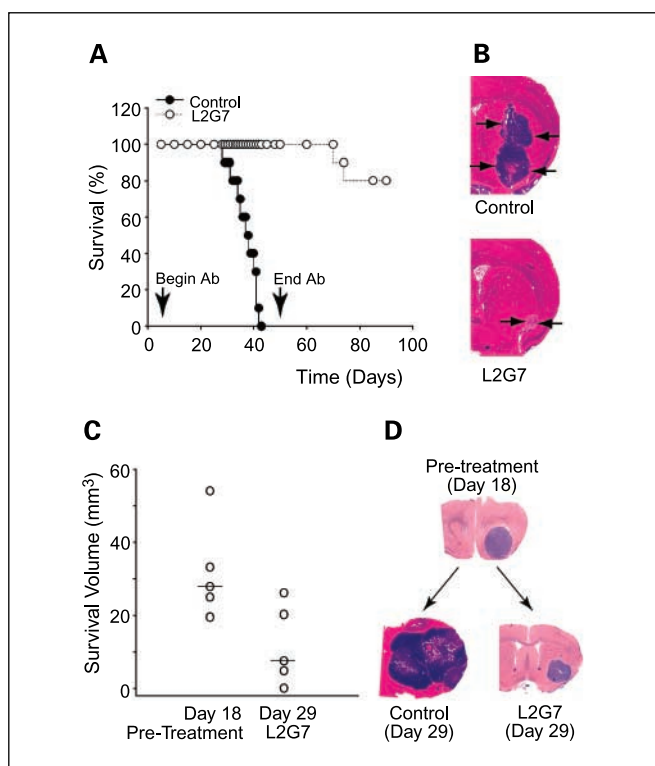


Fig. 4. Inhibition or regression of intracranial U87 glioma xenografts by L2G7. A, U87 tumor cells (10^5 per mouse) were injected intracranially into the caudate/putamen of Scid/Beige mice. Starting and ending, respectively, on days 5 and 52 (arrows); groups of mice (n = 10) were given 100 µg L2G7 or PBS i.p. twice weekly and survival was monitored. B, brain sections from representative mice sacrificed on day 21 after treatment with three doses of 100 µg L2G7 or PBS given i.p. twice weekly, showing the size of U87 intracranial xenografts. C, intracranial U87 tumor volumes in individual mice on day 18 before starting treatment and on day 29 after treatment with three doses of 100 µg L2G7 given i.p. twice weekly. D, brain sections from representative mice on day 18 before treatment and on day 29 after treatment with three doses of 100 µg L2G7 or control mAb given i.p. twice weekly.

Discussion

Targeting the HGF-Met receptor-ligand system is a very promising approach to cancer therapy, supported by strong correlative and preclinical data linking Met activation to the oncogenesis of multiple malignancies (1). However, this concept has not yet been tested clinically because of the difficulty in developing antagonists of the HGF-Met pathway with suitable activity and specificity for testing in humans. The antibody-based approach described here represents a highly rational strategy for overcoming this problem in order to target HGF/Met-associated cancers. To date, the numerous recent advances in antibody-based cancer therapeutics have been limited to systemic malignancies despite the fact that both primary and metastatic brain cancers also express targets amenable to antibody-mediated inhibition. Hence, an especially promising application of the neutralizing anti-HGF mAb characterized here may be to the treatment of gliomas because these tumors commonly express HGF and Met (29, 30).

To our knowledge, the results reported here are the most striking example of therapeutic brain tumor responses from a mAb not linked to a toxin or radionuclide. As a comparison, the anti-VEGF murine mAb A4.6.1, which was later humanized to create the drug Avastin, inhibited the growth of the G55 human glioma by only ~50% to 60% in s.c. xenograft models (17), contrasted with essentially complete growth inhibition and/or regression of the U87 and U118 gliomas by mAb L2G7. In an orthotopic intracranial tumor model, systemic anti-VEGF

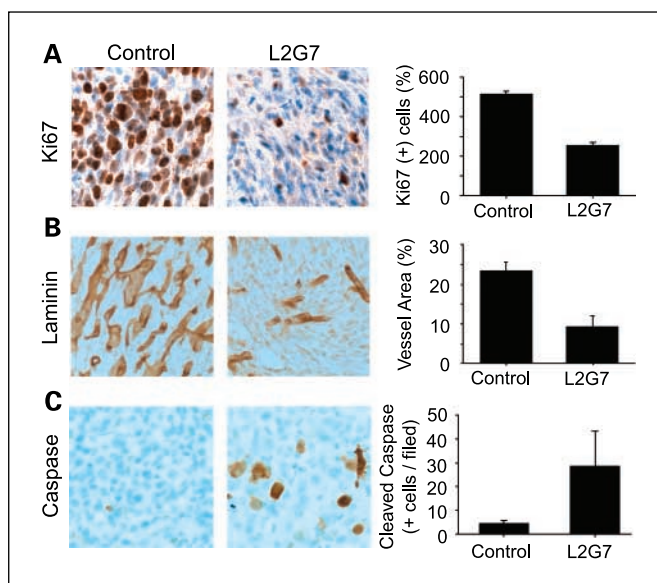


Fig. 5. Histologic analysis of brain sections from mice with U87 intracranial xenografts. The mice were sacrificed on day 29 after treatment of preestablished tumors with three doses of 100 μ g L2G7 or control mAb given i.p. twice weekly. *A*, anti-Ki67 to detect proliferating cells. *B*, anti-laminin to detect blood vessels. *C*, antibody to cleaved caspase-3 to detect apoptotic tumor cell responses.

mAb given simultaneously with G55 glioma cell implantation prolonged animal survival by only 2 to 3 weeks (31). This modest therapeutic effect likely occurred, at least in part, by delaying the initiation of xenograft vascularization, an event that cannot be targeted in patients with preexisting brain tumors. A similar approach used a mAb against a constitutively active mutant epidermal growth factor receptor (EGFRvIII) and three different glioma tumor cell lines engineered to express transgenic EGFRvIII (32). Treatment with the mAb (i.p.) prolonged median survival of mice bearing intracranial tumors of these cell lines by 5, 8, and 39 days, respectively. The therapeutic effect was modest for two of the three cell lines tested despite the fact that the cell lines were specifically constructed to be responsive to the mAb, and treatment was initiated concurrent with tumor cell implantation. Hence, the extent to which these previous reports could be generalized to more natural and stringent brain tumor models or to treatment of humans was left unclear.

In contrast to these reports, the results presented here with anti-HGF L2G7 show that systemic administration of a mAb can be comparably efficacious against intracranial and s.c. HGF-producing xenografts, can induce actual regression of both types of xenografted tumors even in the setting of large pretreatment tumor burden, and can substantially prolong survival of mice bearing natural human glioma xenografts. Hence, in this situation, the blood-brain and blood-tumor barriers do not seem to impede L2G7 efficacy. The pronounced antitumor effects of mAb L2G7 on glioma tumor xenografts are likely due to the unique multifunctional properties of its molecular target HGF, i.e., mitogenic, angiogenic, and cytoprotective (1, 2). The ability of L2G7 to induce glioma regression implicates a cell death response that could result from Fas-mediated apoptosis, which is blocked by HGF binding to Met (33, 34), or from inactivating HGF-induced cytoprotective pathways that involve phosphatidylinositol 3-kinase, Akt, and

nuclear factor κ B intermediates (24, 25). The ability of L2G7 to block the cytoprotective and angiogenic effects of HGF predicts that L2G7 delivered ultimately via systemic or direct intratumoral infusion will potentiate cytotoxic modalities such as γ -radiation and chemotherapy currently used to treat malignant brain tumors (35). Although L2G7 is effective against experimental CNS tumor xenografts, additional experiments are required to determine L2G7 biodistribution and whether L2G7 primarily targets the glioma cells, the tumor vasculature, or both.

The potent antitumor effect of L2G7 was observed on U87 and U118 tumor cells that express cell surface Met and secrete HGF, as is the case for many or most gliomas, to generate an autocrine growth-promoting and cytoprotective loop (30). As predicted, U251 glioma tumor cells that express Met but do not secrete HGF were completely resistant to L2G7 treatment, confirming the specificity of L2G7 antitumor activity. It has been well documented that HGF-dependent tumor cell Met activation can occur in a paracrine manner in tumor types that express Met alone. Indeed, increasing evidence suggests the importance of bidirectional interactions between human tumor cells and neighboring stromal cells such as fibroblasts and endothelial cells (36), so that factors secreted by the tumor may induce the secretion of HGF from stromal cells, which in turn stimulates tumor growth. Hence, in human patients, the L2G7 mAb (in a humanized form) has the potential to be effective against Met+/HGF- tumors as well as Met+/HGF+ tumors. The efficacy of mAb L2G7 against such host-derived HGF-dependent paracrine tumor-promoting pathways cannot be readily tested in standard mouse xenograft models, both because mouse HGF, at most, weakly activates human Met (37–39), and because L2G7 does not bind and neutralize mouse HGF. However, testing this application of anti-HGF therapeutics may be feasible using recently described immunodeficient mice transgenic for human HGF that have been shown to stimulate the growth of Met+/HGF- tumor xenografts (40). On the other hand, it should be pointed out that Met activation in tumor cells could occur through HGF-independent pathways (7). Thus, some glioma tumors, such as U251, which overexpress Met, may be activated in an HGF-independent manner. Such tumors are unlikely to respond to L2G7 treatment. Furthermore, even some Met+/HGF+ tumors may not respond well to HGF-targeted therapy due to the use of alternative protumorigenic pathways.

The present study shows that a single mAb delivered systemically can have dramatic inhibitory effects on intracranial tumor growth and further supports the significance of HGF as an important mediator of oncogenesis of gliomas and potentially other tumor types. Our study suggests that recent encouraging results with antagonists of growth factors and their receptors in the treatment of breast, colon, and lung cancer may be extended to noninvasive treatment of clinically intractable CNS malignancies by using an HGF-blocking mAb either alone or with other cytotoxic therapies.

Acknowledgments

We thank Drs. C. Queen and R. Abounader for their support and careful review of the manuscript, and W. Jiang for assistance with the subcutaneous xenograft animal studies.

References

1. Birchmeier C, Birchmeier W, Gherardi E, Vande Woude GF. Met, metastasis, motility and more. *Nat Rev Mol Cell Biol* 2003;4:915–25.
2. Trusolino L, Comoglio PM. Scatter-factor and semaphorin receptors: cell signalling for invasive growth. *Nat Rev Cancer* 2002;4:289–98.
3. Schmidt C, Bladt F, Goedecke S, et al. Scatter factor/hepatocyte growth factor is essential for liver development. *Nature* 1995;373:699–702.
4. Uehara Y, Minowa O, Mori C, et al. Placental defect and embryonic lethality in mice lacking hepatocyte growth factor/scatter factor. *Nature* 1995;373:702–5.
5. Matsumoto K, Nakamura T. HGF: its organotrophic role and therapeutic potential. *Ciba Found Symp* 1997;212:198–211.
6. Maulik G, Shrikhande A, Kijima T, Ma PC, Morrison PT, Salgia R. Role of the hepatocyte growth factor receptor, c-Met, in oncogenesis and potential for therapeutic inhibition. *Cytokine Growth Factor Rev* 2002;13:41–59.
7. Danilkovitch-Miagkova A, Zbar B. Dysregulation of Met receptor tyrosine kinase activity in invasive tumors. *J Clin Invest* 2002;109:863–7.
8. Abounader R, Lal B, Luddy C, et al. *In vivo* targeting of SF/HGF and c-met expression via U1snRNA/ribozymes inhibits glioma growth and angiogenesis and promotes apoptosis. *FASEB J* 2002;16:108–10.
9. Michieli P, Mazzone M, Basilico C, et al. Targeting the tumor and its microenvironment by a dual-function decoy Met receptor. *Cancer Cell* 2004;6:61–73.
10. Date K, Matsumoto K, Kuba K, Shimura H, Tanaka M, Nakamura T. Inhibition of tumor growth and invasion by a four-kringle antagonist (HGF/NK4) for hepatocyte growth factor. *Oncogene* 1998;17:3045–54.
11. Cao B, Su Y, Oskarsson M, et al. Neutralizing monoclonal antibodies to hepatocyte growth factor/scatter factor (HGF/SF) display antitumor activity in animal models. *Proc Natl Acad Sci U S A* 2001;98:7443–8.
12. No D, Yao TP, Evans RM. Ecdysone-inducible gene expression in mammalian cells and transgenic mice. *Proc Natl Acad Sci U S A* 1996;93:3346–51.
13. Chuntharapai A, Kim KJ. Generation of monoclonal antibodies to chemokine receptors. *Methods Enzymol* 1997;288:15–27.
14. Borsset M, Waage A, Sundan A. Hepatocyte growth factor reverses the TGF- β -induced growth inhibition of CCL-64 cells. A novel bioassay for HGF and implications for the TGF- β bioassay. *J Immunol Methods* 1996;189:59–64.
15. Xin X, Yang S, Ingle G, et al. Hepatocyte growth factor enhances vascular endothelial growth factor-induced angiogenesis *in vitro* and *in vivo*. *Am J Pathol* 2001;15:1111–20.
16. Choi C, Xu X, Oh JW, et al. Fas-induced expression of chemokines in human glioma cells: involvement of extracellular signal-regulated kinase 1/2 and p38 mitogen-activated protein kinase. *Cancer Res* 2001;61:3084–91.
17. Kim KJ, Li B, Winer J, et al. Inhibition of vascular endothelial growth factor-induced angiogenesis suppresses tumor growth *in vivo*. *Nature* 1993;362:841–4.
18. Weidner KM, Sachs M, Birchmeier W. The Met receptor tyrosine kinase transduces motility, proliferation, and morphogenic signals of scatter factor/hepatocyte growth factor in epithelial cells. *J Cell Biol* 1993;121:145–54.
19. Lokker NA, Mark MR, Luis EA, et al. Structure-function analysis of hepatocyte growth factor: identification of variants that lack mitogenic activity yet retain high affinity receptor binding. *EMBO J* 1992;11:2503–10.
20. Hartmann G, Naldini L, Weidner KM, et al. A functional domain in the heavy chain of scatter factor/hepatocyte growth factor binds the c-Met receptor and induces cell dissociation but not mitogenesis. *Proc Natl Acad Sci U S A* 1992;89:11574–8.
21. Grant DS, Kleinman HK, Goldberg ID, et al. Scatter factor induces blood vessel formation *in vivo*. *Proc Natl Acad Sci U S A* 1993;90:1937–41.
22. Schmidt NO, Westphal M, Hagel C, et al. Levels of vascular endothelial growth factor, hepatocyte growth factor/scatter factor and basic fibroblast growth factor in human gliomas and their relation to angiogenesis. *Int J Cancer* 1999;84:10–8.
23. Saucier C, Khoury H, Lai KM, et al. The Shc adaptor protein is critical for VEGF induction by Met/HGF and ErbB2 receptors and for early onset of tumor angiogenesis. *Proc Natl Acad Sci U S A* 2004;101:2345–50.
24. Bowers DC, Fan S, Walter KA, et al. Scatter factor/hepatocyte growth factor activates AKT and protects against cytotoxic death in human glioblastoma via PI3-kinase and AKT-dependent pathways. *Cancer Res* 2000;60:4277–83.
25. Fan S, Gao M, Meng Q, et al. Role of NF- κ B signalling in hepatocyte growth factor/scatter factor mediated cell protection. *Oncogene* 2005;24:1749–66.
26. Weller M, Frei K, Groscurth P, Krammer PH, Yonekawa Y, Fontana A. Anti-Fas/APO-1 antibody-mediated apoptosis of cultured human glioma cells. Induction and modulation of sensitivity by cytokines. *J Clin Invest* 1994;94:954–64.
27. Rich JN, Bigner DD. Development of novel targeted therapies in the treatment of malignant glioma. *Nat Rev Drug Discov* 2004;3:430–46.
28. Bendell JC, Domchek SM, Burstein HJ, et al. Central nervous system metastases in women who receive trastuzumab-based therapy for metastatic breast carcinoma. *Cancer* 2003;97:2972–7.
29. Rosen EM, Laterra J, Joseph A, et al. Scatter factor expression and regulation in human glial tumors. *Int J Cancer* 1996;67:248–55.
30. Koochekpour S, Jeffers M, Rulong S, et al. Met and hepatocyte growth factor/scatter factor expression in human gliomas. *Cancer Res* 1997;57:5391–8.
31. Rubenstein JL, Kim J, Ozawa T, et al. Anti-VEGF antibody treatment of glioblastoma prolongs survival but results in increased vascular cooption. *Neoplasia* 2000;2:306–14.
32. Mishima K, Johns TG, Luwor RB, et al. Growth suppression of intracranial xenografted glioblastomas overexpressing mutant epidermal growth factor receptors by systemic administration of monoclonal antibody (mAb) 806, a novel monoclonal antibody directed to the receptor. *Cancer Res* 2001;61:5349–54.
33. Wang X, DeFrances MC, Dai Y, et al. A mechanism of cell survival: sequestration of Fas by the HGF receptor Met. *Mol Cell* 2002;9:411–21.
34. Huh CG, Factor VM, Sanchez A, Uchida K, Conner EA, Thorgeirsson SS. Hepatocyte growth factor/c-met signaling pathway is required for efficient liver regeneration and repair. *Proc Natl Acad Sci U S A* 2004;101:4477–82.
35. Lal B, Xia S, Abounader R, Laterra J. Targeting the c-Met pathway potentiates glioblastoma responses to γ -radiation. *Clin Cancer Res* 2005;11:4479–86.
36. Bogenrieder T, Herlyn M. Axis of evil: molecular mechanisms of cancer metastasis. *Oncogene* 2003;22:6524–36.
37. Bhargava M, Joseph A, Knesel J, et al. Scatter factor and hepatocyte growth factor: activities, properties, and mechanism. *Cell Growth Differ* 1992;3:11–20.
38. Bussolino F, Di Renzo MF, Ziche M, et al. Hepatocyte growth factor is a potent angiogenic factor, which stimulates endothelial cell motility and growth. *J Cell Biol* 1992;119:629–41.
39. Rong S, Bodescot M, Blair D, et al. Tumorigenicity of the met proto-oncogene and the gene for hepatocyte growth factor. *Mol Cell Biol* 1992;12:5152–8.
40. Zhang YW, Su Y, Lanning N, et al. Enhanced growth of human met-expressing xenografts in a new strain of immunocompromised mice transgenic for human hepatocyte growth factor/scatter factor. *Oncogene* 2005;24:101–6.

Clinical Cancer Research

Systemic anti-hepatocyte growth factor monoclonal antibody therapy induces the regression of intracranial glioma xenografts.

K Jin Kim, Lihong Wang, Yi-Chi Su, et al.

Clin Cancer Res 2006;12:1292-1298.

Updated version Access the most recent version of this article at:
<http://clincancerres.aacrjournals.org/content/12/4/1292>

Cited articles This article cites 40 articles, 15 of which you can access for free at:
<http://clincancerres.aacrjournals.org/content/12/4/1292.full#ref-list-1>

Citing articles This article has been cited by 34 HighWire-hosted articles. Access the articles at:
<http://clincancerres.aacrjournals.org/content/12/4/1292.full#related-urls>

E-mail alerts [Sign up to receive free email-alerts](#) related to this article or journal.

Reprints and Subscriptions To order reprints of this article or to subscribe to the journal, contact the AACR Publications Department at pubs@aacr.org.

Permissions To request permission to re-use all or part of this article, use this link
<http://clincancerres.aacrjournals.org/content/12/4/1292>.
Click on "Request Permissions" which will take you to the Copyright Clearance Center's (CCC) Rightslink site.